Synthesis and Characterization of LDHs/PMMA Nanocomposites: Effect of Two Different Intercalated Anions on the Mechanical and Thermal Properties

Telma Nogueira,[1] Rodrigo Botan,[1] Fernando Wypych,[2] Liliane Lona[1]

[1]*School of Chemical Engineering, University of Campinas, Campinas, S.P., Brazil*
[2]*Chemistry Department, Federal University of Paraná, Curitiba, P.R., Brazil*

Received 11 April 2011; accepted 5 July 2011
DOI 10.1002/app.35213
Published online 21 October 2011 in Wiley Online Library (wileyonlinelibrary.com).

ABSTRACT: Poly(methyl methacrylate) (PMMA)/layered double hydroxides (LDH) nanocomposites were synthesized by *in situ* bulk polymerization. The LDHs were synthesized by coprecipitation method. Eight LDHs having different compositions were produced, varying the divalent/trivalent cations (Zn/Al, Mg/Fe), the ratio between these cations (2: 1 and 4: 1) and the LDH intercalated anions (dodecyl sulfate and laurate). The LDH percentage (wt %) in the PMMA was fixed at 1%. The thermal properties of the nanocomposites were evaluated by thermal analysis (thermogravimetric—TGA and differential scanning calorimetry—DSC). Most of the nanocomposites presented higher thermal resistance than PMMA and the best results were presented by the following nanocomposites: PMMA/(Zn/Al 2: 1 laurate) and PMMA/(Zn/Al 4: 1 laurate). The dynamic mechanical properties of the nanocomposites were investigated and compared to those obtained for PMMA. It was noticed that PMMA/(Mg/Fe 4: 1 laurate) nanocomposite presented an elastic modulus 2.2 times higher than PMMA at 40°C. This investigation demonstrated that the addition of low concentrations of selected LDHs can enhance some desired properties of PMMA. © 2011 Wiley Periodicals, Inc. J Appl Polym Sci 124: 1764–1770, 2012

Key words: nanocomposites; mechanical properties; polymer synthesis and characterization

INTRODUCTION

Nowadays, plastics have been used as substitutes for many products like wood, paper, glass, etc. However, the use of plastic still presents some limitations. In the packaging industry, for example, certain foods (tomato products and beer) are sensitive to oxygen and cannot be stored in plastic packages due to oxygen permeability. In the automobile industry, low stiffness, tensile strength, and the heat deformation have limited the use of plastics in their applications.[1] Trying to overcome these plastics properties limitations, some scientific groups are studying the properties of polymer hybrid compounds.[2–6]

Among all of the potential nanocomposite precursors, those based on clay minerals and based on layered silicates have been more widely investigated, probably because the raw clay materials are easily available and their intercalation chemistry has been studied for a long time.[7]

Layered double hydroxides (LDHs), also known as anionic clays, are a special group of layered hydroxides.[8] These compounds (anionic clays), are very simple and inexpensive to synthesize, and there is a wide range of LDHs with a highly defined composition that can be produced. LDHs, also known as hydrotalcite-like compounds, present structures that derive from brucite ($Mg(OH)_2$). Brucite structure is composed by regular octahedron wherein its center has magnesium cations and their vertices have hydroxyl groups. These octahedra share edges forming infinite bidimensional layers. In LDHs some divalent cations are replaced by trivalent cations generating a positive charge that is balanced by the intercalation of exchangeable anions, generating a compound with a generic formula $[M^{+2}_{1-x}M^{+3}_{x}(OH)_2]^{x+}(A^{n-})_{x/n}.yH_2O$. However, since the LDH's surface is hydrophilic, it needs to be organically modified to become hydrophobic and therefore the LDH's layers could be dispersed in the polymeric matrix. Organic modifications have two major objectives: first, an appropriate organic species reduces the hydrophilicity of the clay layers and enhances compatibility between the layers and the polymer matrix; second, larger gallery spacing hinders electrostatic interactions between the layers and makes it easier to achieve exfoliation of the layered crystals into single layers.[9,10]

Correspondence to: T. Nogueira (telma.nogueira@gmail.com).

Contract grant sponsor: CNPq (Conselho Nacional de Desenvolvimento Científico e Tecnológico) [National Council for Scientific and Technological Development].

The objective of the present work is to compare the effect of LDHs with different anions (dodecyl sulfate and laurate) on the dynamic mechanical and thermal properties of the PMMA nanocomposites obtained by *in situ* bulk polymerization. There are few studies in open literature about this theme.[11–13] Tseng et al.[11] studied the effect of LDH-amino benzoate and LDH-carbonate on the mechanical and thermal properties of epoxy nanocomposites. In the Berti et al.[12] study, the LDH was modified by 4-sulfobenzoate, dimethyl 5-sulfo isophthalate, and dodecyl sulfate and the matrix polymeric was poly (butylene terephtalate). Nyambo et al.[13] studied the effect of different LDHs-alkyl carboxylates on the fire-retardancy of PMMA and they have shown that the addition of the LDHs improved the thermal stability for all filler loadings. They also evaluated some mechanical properties of the nanocomposites and noticed that they presented a lower tensile strength than PMMA. Although they have already studied the effect of different LDH-intercalated anions, they prepared the nanocomposites by melt-blending process, and they only evaluated one pair of divalent-trivalent cations (Mg/Al) in only one ratio (2: 1). In this work it was possible to obtain some nanocomposites that exhibited excellent performance in thermal and dynamic mechanical properties.

EXPERIMENTAL

Materials and methods

Sodium dodecyl sulfate (NaDDS) (FMaia), lauric acid (Vetec), tert-butylperoxy 2-ethylhexyl carbonate (TBEC; σ-Aldrich, 95%), sodium hydroxide, calcium chloride (Ecibra), zinc chloride, aluminum chloride, magnesium chloride (Ecibra), ferric chloride (Synth) were of analytical grade and used as received. Methyl methacrylate (σ-Aldrich, 99%) was washed three times with a 10 w/v % sodium hydroxide solution, and then, three times with deionized water, and finally dehydrated over calcium chloride.

Synthesis of LDHs

The LDHs were prepared by coprecipitation method. The synthesis of LDHs was performed under nitrogen atmosphere to avoid the presence of carbonates between the LDHs layers. After deciding the proportions between the cations, the required amounts of chlorides, sodium hydroxide, and sodium dodecyl sulfate or lauric acid were weighed and dissolved in deionized water. The sodium dodecyl sulfate or lauric acid solution was poured into a reactor, the salts solutions were mixed and slowly added to the reactor. To maintain the pH near 10 a solution of sodium hydroxide was also added to the reactor. The reaction was carried out at 35°C and the final mixture was reacted at a pH near 8, for 12 h under dynamic flow of nitrogen. The mixture was centrifuged at 4000 rpm for 12 min, for the removal of supernatant liquid, this process was repeated for five times. The solids were dried at 45°C until constant weight.

Preparation of LDHs/PMMA nanocomposites

The LDHs/PMMA nanocomposites were prepared by *in situ* bulk polymerization. More details can be seen on our previous studies.[14,15] Because of the preliminary investigations of the effect of the percentage of filler into different polymeric matrices, the weight fraction of LDH was fixed in 1% (w/w). Methyl methacrylate (MMA; 30 mL), TBEC initiator (0.04 mol L^{-1}) and LDH were weighed and stirred for 1 h at room temperature and the mixture was poured into glass ampoules. These ampoules were degassed by three freeze/pump/thaw cycles under vacuum and after they were torch-sealed. The polymerizations were carried out in a circulator bath, containing silicone oil, with temperature control, at 95°C. After 2 h of reaction, at 100% of monomer conversion, the ampoules were withdrawn, broken and the samples were stored.

Characterizations of nanocomposites

The X-ray diffraction measurements were performed with a Shimadzu-XRD 7000 diffractometer, using Cu Kα radiation (λ = 1.5406 Å), at a rate of 2° min^{-1}, operating at 40 kV and 30 mA. FTIR analyses were performed in the Spectrum One Perkin–Elmer equipment, in a wavenumber range of 400–4000 cm^{-1}. Thermogravimetric analysis (TGA) was obtained on a Universal V2.3C TA Instrument. Samples were heated from 30 to 700°C, with a heating rate of 20°C min^{-1} on oxidant atmosphere (oxygen rate of 100 mL min^{-1}). DMA analyses were performed using a dynamic mechanical analyzer from Netzsch, type DMA 242, using the sample holder for three-point free bending mode, with a frequency of 1 Hz, at a heating rate of 2°C min^{-1} and in the temperature range of 25–200°C. The samples of the nanocomposites had cylindrical geometry with 4.75 mm in diameter by 35 mm in length. Differential scanning calorimetric analysis (DSC) were performed using the Mettler Toledo DSC 823e equipment, under oxygen flow (50 mL min^{-1}) with a heating rate of 20°C min^{-1} and the temperature ranged from 25 to 500°C.

RESULTS AND DISCUSSION

In this work eight different LDHs were synthesized as seen in Table I. LDHs were produced with different compositions varying the divalent/trivalent

TABLE I
LDHs Produced by Coprecipitation Method

Layered double hydroxides
Zn/Al 2: 1 dodecyl sulfate
Zn/Al 4: 1 dodecyl sulfate
Mg/Fe 2: 1 dodecyl sulfate
Mg/Fe 4: 1 dodecyl sulfate
Zn/Al 2: 1 laurate
Zn/Al 4: 1 laurate
Mg/Fe 2: 1 laurate
Mg/Fe 4: 1 laurate

cations, divalent/trivalent cations ratios and intercalated anions to verify how the different metals composition, the layers charge density, and the intercalated anionic specie affects the PMMA nanocomposites properties. The X-ray diffraction patterns of LDHs (intercalated by DDS and Laurate) and PMMA nanocomposites (containing DDS and Laurate) are shown in Figures 1–4, respectively. Using this technique it is possible to determine the basal spacing from the higher order basal reflections by using Bragg's law, the results are presented in Figures 1 and 2. The reported thickness of the brucite-like LDH layer is 4.8 Å.[10] Figures 1 and 2 show that the basal distances of all LDHs are consistent with the intercalation of DDS and laurate between the layers. The anion intercalation is important because hydrotalcite presents a small interlayer distance which prevents the intercalation of monomer or polymer chains. Furthermore, the hydrophilic surface of the LDH layers is incompatible with hydrophobic polymer molecules. For these two reasons, monomer and polymer molecules cannot easily penetrate between the LDH layers nor can the LDH layers be easily homogeneously dispersed in the hydrophobic polymer matrix.[16] It can be seen in Figure 1 (Laurate intercalated LDHs) and Figure 2 (all the LDHs) that some LDHs present an additional series of basal reflections, which can indicate that the

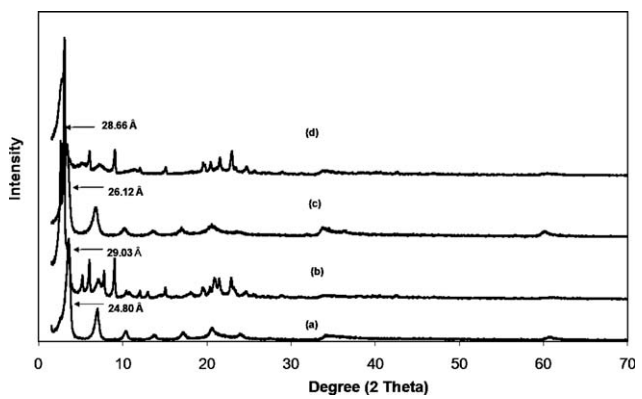

Figure 1 X-ray diffraction patterns: (a) Zn/Al 2: 1 DDS, (b) Zn/Al 2: 1 Laurate, (c) Zn/Al 4: 1 DDS, (d) Zn/Al 4: 1 Laurate.

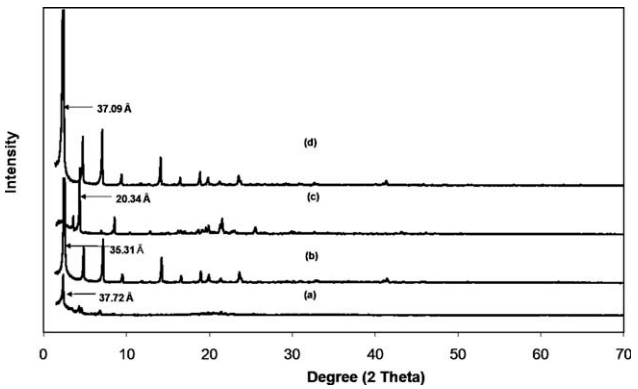

Figure 2 X-ray diffraction patterns: (a) Mg/Fe 2: 1 DDS, (b) Mg/Fe 2: 1 Laurate, (c) Mg/Fe 4: 1 DDS, (d) Mg/Fe 4: 1 Laurate.

samples are contaminated by lauric acid or dodecyl sulfate sodium salt.

Figures 3 and 4 show that PMMA presents two broad diffractions bands 15° and 30° (2 theta) attributed to semicrystaline state of this polymer. These two contributions are observed in the case of the as-made nanocomposites, showing that, independently of the filler content, a similar crystallinity is reached.[5] X-ray diffraction patterns of the nanocomposites shown only two broad and low intensity diffraction peaks in the nanocomposites PMMA/(Zn/Al 2: 1 DDS) [peak at 28 Å in Fig. 3(b)] and PMMA/(Zn/Al 2: 1 laurate) [peak at 36 Å in Fig. 3(c)]. As raw Zn: Al 2: 1 DDS and Zn: Al 2: 1 laurate shown peak at 24.8 and 29 Å, respectively, this new peaks can indicate the intercalation of the polymers into the LDH galleries.

The absence of any peak in all the other compositions can indicate the exfoliation of the LDHs layered crystals. Another possibility is the difficulty to observe diffraction peaks of the LDHs with as smaller concentration as 1 wt %.[7]

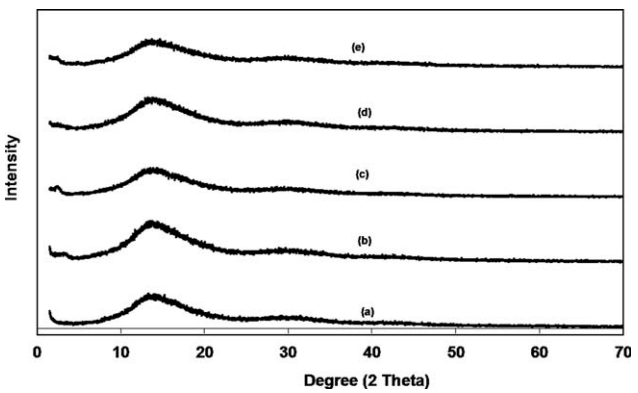

Figure 3 X-ray diffraction patterns of PMMA (a) and PMMA nanocomposites (b–e), (b) Zn: Al 2: 1 DDS, (c) Zn/Al 2: 1 Laurate, (d) Zn/Al 4: 1 DDS, (e) Zn/Al 4: 1 Laurate.

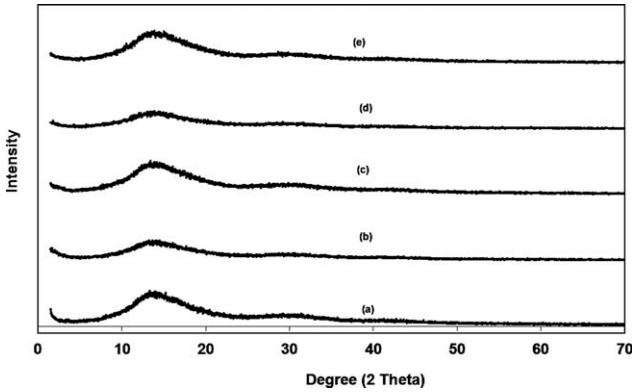

Figure 4 X-ray diffraction patterns of PMMA (a) and PMMA nanocomposites (b–e), (b) Mg/Fe 2: 1 DDS, (c) Mg/Fe 2: 1 Laurate, (d) Mg/Fe 4: 1 DDS, (e) Mg/Fe 4: 1 Laurate.

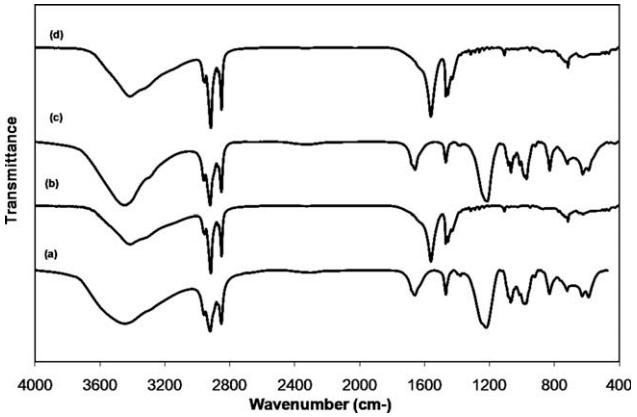

Figure 6 FTIR spectra of LDHs, (a) Mg/Fe 2: 1 DDS, (b) Mg/Fe 2: 1 Laurate, (c) Mg/Fe 4: 1 DDS, (d) Mg/Fe 4: 1 Laurate.

FTIR spectra of LDHs are shown in Figures 5 and 6. It can be observed for all the LDHs, peaks at 2800–3000 cm^{-1} that correspond to asymmetric and symmetric stretching vibration of methyl and methylene groups which can prove that the DDS and Laurate anions have been intercalated between LDHs layers. A common LDH broad band occurs near 3500 cm^{-1} and it can correspond to stretching vibration of hydroxyl group. The samples containing DDS presented a band near 1640 cm^{-1} that can indicate the presence of water, since the bending vibration of OH is present in this region. They also presented peaks at 1220, 1060, and 630 cm^{-1} that are attributed to stretching vibration of S=O and C—S group, respectively, confirming the DS intercalation. All the LDHs spectra presented a peak at 1470 cm^{-1} that can indicate that carbonate also is present in the interlayer space. In Figure 5 the Laurate-LDH presented two peaks at 1540 and 1410 cm^{-1} associated to asymmetric and symmetric carboxylate stretching vibration which can indicate the laurate presence. In Figure 6(b,d) the presence of the laurate in the interlayer is associated to the peak at near 1570 cm^{-1} that correspond to asymmetric stretching vibration of carboxylate. The sample Zn/Al 2: 1 Laurate presented a peak at 1600 cm^{-1} that can be associated to carbonyl stretching vibration of lauric acid, as contaminant or due to H-bonding of the free acid with carboxylate and/or pendant layer hydroxide groups.[17] These results and those of X-ray diffraction confirm the presence of contaminants. The bands that had occurred below 800 cm^{-1} can be attributed to M—O and O—M—O vibration modes, where M = Zn, Al, Mg, and Fe.

Figures 7 and 8 show FTIR spectra for PMMA and the nanocomposites synthesized. It can be noticed that the nanocomposites exhibit a spectra with PMMA characteristics absorption bands. Indeed, the absorption bands at 1729 and 3438 cm^{-1} correspond to the carbonyl group. It is difficult to attribute absorption bands to the LDHs because there is a superimposition of PMMA and LDHs bands and peaks, this happens because most of their characteristics bands and peaks occur in the same region. The

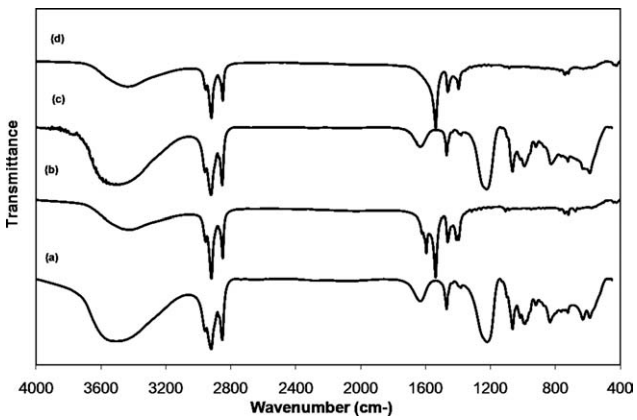

Figure 5 FTIR spectra of LDHs, (a) Zn: Al 2: 1 DDS, (b) Zn/Al 2: 1 Laurate, (c) Zn/Al 4: 1 DDS, (d) Zn/Al 4: 1 Laurate.

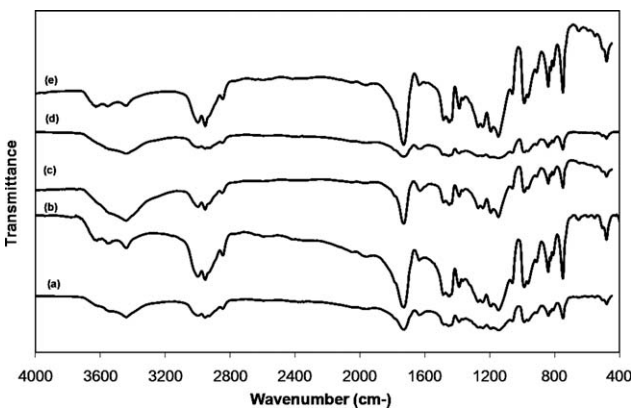

Figure 7 FTIR spectra of PMMA and PMMA nanocomposites, (a) PMMA, (b) Zn/Al 2: 1 DDS, (c) Zn/Al 2: 1 Laurate, (d) Zn/Al 4: 1 DDS, (e) Zn/Al 4: 1 Laurate.

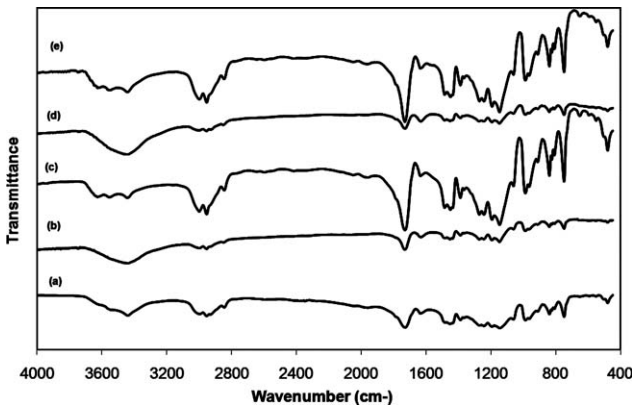

Figure 8 FTIR spectra of PMMA and PMMA nanocomposites, (a) PMMA, (b) Mg/Fe 2: 1 DDS, (c) Mg/Fe 2: 1 Laurate, (d) Mg/Fe 4: 1 DDS, (e) Mg/Fe 4: 1 Laurate.

overtone of the carbonyl 1715 cm^{-1} absorption may appear around 3430 cm^{-1}, and may be confused with the hydroxyl absorption.[18] Besides, PMMA and LDHs present many peaks and bands common to both as those related to hydrocarbon stretching vibration as at 2969 and 2861 cm^{-1} that are associated with asymmetric and symmetric stretching vibration of methyl and methylene group, respectively. A strong peak at 1150 cm^{-1} belonging to the group of bands between 1270 and 990 cm^{-1} originate from the C—O stretching vibrations.[19]

Figure 9 shows the thermal decomposition processes for PMMA and PMMA/LDH nanocomposites. The onset degradation temperature T_{10} (temperature at which a 10% loss of mass occurs), the mid-point degradation temperature T_{50} (temperature at which a weight loss of 50% is lost), and T_d (temperature at which the polymer/nanocomposite degradation occurs) are shown in Table II. From TGA curves and summary of TGA data, it can be seen that most of the nanocomposites presented an initial degradation rate very similar to PMMA. However, the nanocomposites composed by Zn/Al 2: 1 Laurate and Zn/Al 4: 1 Laurate presented slower onset degradation rates (about 16°C higher) than pure PMMA. At 50% weight loss, almost all the nanocompostites had an enhancement on thermal stability compared to PMMA and, for the best result, T_{50} increased from 313°C (PMMA) to 356°C (PMMA/(Zn/Al 2: 1 laurate)). Almost all the nanocomposites had total degradation temperatures higher than PMMA and the Zn/Al 4: 1 laurate/PMMA nanocomposite presented total decomposition temperature 77°C higher than the one obtained for pure PMMA. These results can be attributed to the good LDH dispersion and/or chemical bonds between the LDHs and the polymeric matrix which could enhance the thermal stability of the nanocomposites. The enhancement may be explained in two ways. First, the inorganic LDH layers have a much higher thermal resistance than the organic PMMA molecules. Second, the excellent barrier property of homogeneously dispersed LDH layers prevents the migration of some small volatile molecules from the inner matrix to the surface.[10]

TABLE II
Summary of TGA Data for PMMA and PMMA Nanocomposites

Sample	T_{10} (°C)	T_{50} (°C)	T_d (°C)
PMMA	248	313	413
Zn/Al 2: 1 DDS/PMMA	245	302	430
Zn/Al 4: 1 DDS/PMMA	248	314	433
Mg/Fe 2: 1 DDS/PMMA	252	338	410
Mg/Fe 4: 1 DDS/PMMA	233	317	413
Zn/Al 2: 1 laurate/PMMA	263	356	487
Zn/Al 4: 1 laurate/PMMA	264	350	490
Mg/Fe 2: 1 laurate/PMMA	245	335	430
Mg/Fe 4: 1 laurate/PMMA	246	334	423

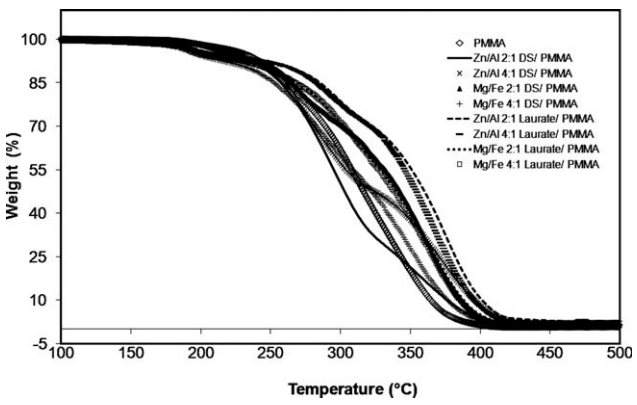

Figure 9 TGA curves to PMMA and PMMA nanocomposites.

Radical polymerized PMMA usually presents three steps of thermal decomposition. The steps are cleavage of the head-to-head linkages, initiation of depolymerization at the unsaturated end group, and random scission of the main chain.[20] Table III presents the temperatures of PMMA and nanocomposites thermal degradation steps. In this study the first stage of degradation (head-to-head linkage) occurred at 166°C. It was also reported that, for PMMA oligomer the head-to-head degradation might initiate at about 195°C.[21] The unsaturated end group degradation occurred at about 310°C. The last stage, associated to main chain decomposition, occurred at about 392°C. It can be noticed that all the nanocomposites also presented three-step degradation, with degradation temperatures of each stage very similar to those found to PMMA. The obtained results indicate that the LDH incorporation on PMMA matrix did not alter its thermal degradation mechanism. Because of the lower concentration, degradation steps related to LDHs were not observed.

TABLE III
Thermal Decomposition Stages for the PMMA and PMMA Nanocomposites

	Steps of PMMA thermal decomposition		
Sample	Cleavage of head-to-head linkages	Degradation of unsaturated end groups	Scission of PMMA chains
PMMA	166/202	310	392
PMMA/(Zn/Al 2: 1 DDS)	169/203	314	394
PMMA/(Zn/Al 4: 1 DDS)	196	311	379
PMMA/(Mg/Fe 2: 1 DDS)	193	306	381
PMMA/(Mg/Fe 4: 1 DDS)	164/197	307	384
PMMA/(Zn/Al 2: 1 laurate)	153/201	306	401
PMMA/(Zn/Al 4: 1 laurate)	171/200	308	384
PMMA/(Mg/Fe 2: 1 laurate)	168/202	307	395
PMMA/(Mg/Fe 4: 1 laurate)	198	306	385

Dynamic mechanical properties were obtained using a dynamic mechanical analyzer. Figure 10 shows the elastic modulus as a function of the temperature for PMMA and the nanocomposites produced. Table IV presents elastic modulus for PMMA and PMMA/LDH nanocomposites (at 40 and 100°C) and glass transition temperature. Glass transition temperature was identified through tan δ peak in tan δ versus temperature curve. The E' value is directly related to the ability of the material to tolerate mechanical loads with recoverable strain and it is similar to flexural modulus.[22] Conceptually, inorganic organic composites are often expected to become stiff and more brittle upon incorporation of inorganic fillers.[11] Figure 10 shows that most of the nanocomposites presented higher elastic modulus than PMMA at the studied temperature range, and at about 110°C all the nanocomposites presented an abrupt decrease on elastic modulus because most of them reached the glass transition temperature. From this temperature, the nanocomposites stiffness began to decrease and then their mechanical properties were adversely affected. The nanocomposite PMMA/(Mg/Fe 4: 1 laurate) presented the best result and the ratio between its elastic modulus and the PMMA elastic modulus was 2.2 at 40°C and 3.6 at 100°C. As previously observed[12] the elastic modulus that drops in almost all the nanocomposites was lower than the one for PMMA. These results can prove that few percent of some inorganic reinforcements are able to enhance remarkably this mechanical property.

The results of Table IV shows that for some nanocomposites the values of glass transition temperatures shift from 112°C for PMMA to 130°C to PMMA/(Zn/Al 4: 1 DDS). The decrease in the chain mobility which is associated to an increase in T_g results usually of intercalated or exfoliated nanocomposite where chemical binding, weak as hydrogen bond or strong as covalent is arising between the filler and polymer chain.[23]

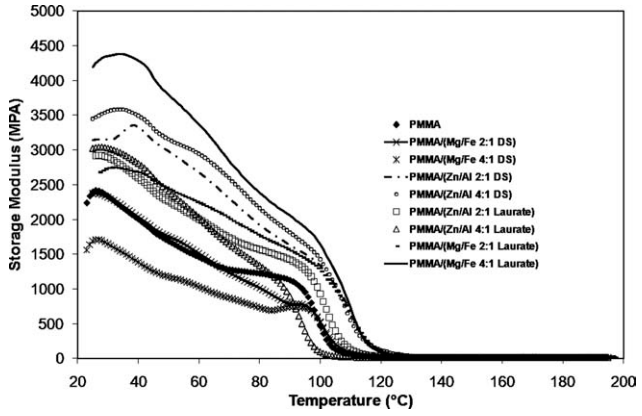

Figure 10 Storage modulus as a function of temperature for PMMA and all the nanocomposites.

CONCLUSIONS

In the present work, a variety of LDHs were synthesized by coprecipitation method. All the inorganic compounds presented a basal spacing consistent with the intercalation of laurate and DDS anions

TABLE IV
Storage Modulus at 40 and 100°C and Glass Transition Temperature for PMMA and the Nanocomposites

	Storage modulus at 40°C	Storage modulus at 100°C	Glass transition temperature (°C)
PMMA	1998	460	112
PMMA/(Zn/Al 2: 1 DDS)	3329	1334	126
PMMA/(Zn/Al 4: 1 DDS)	3493	1426	130
PMMA/(Mg/Fe 2: 1 DDS)	2035	528	114
PMMA/(Mg/Fe 4: 1 DDS)	1386	517	115
PMMA/(Zn/Al 2: 1 Laurate)	2597	928	114
PMMA/(Zn/Al 4: 1 laurate)	2805	99	104
PMMA/(Mg/Fe 2: 1 laurate)	2676	1248	124
PMMA/(Mg/Fe 4: 1 Laurate)	4288	1645	124

between the LDH layers. Nanocomposites were produced by *in situ* bulk polymerization. The X-ray diffraction patterns of the nanocomposites have shown only small diffractions peaks in two different compositions (PMMA/(Zn/Al 2: 1 DDS) and PMMA/(Zn/Al 2: 1 laurate)), which can be attributed to the intercalation of PMMA molecules between the LDH layers. In all other samples, the absence of peaks related to the LDHs can be a strong evidence of LDH exfoliation on the PMMA matrix. TGA curves evidenced that some nanocomposites showed an improvement on thermal stability when compared to PMMA, which can be attributed to LDHs thermal resistance and barrier properties. The best results were observed for the nanocomposites PMMA/(Zn/Al 2: 1 laurate) and PMMA/(Zn/Al 4: 1 laurate). The steps of thermal degradation of all the nanocomposites were investigated by DSC. Results indicated that nanocomposites presented thermal degradation mechanisms similar to those found for PMMA. Most of the nanocomposites presented higher elastic modulus than those found for PMMA, and the nanocomposite that presented better dynamic mechanical property was PMMA/(Mg/Fe 4: 1 laurate).

These results can demonstrate that it is possible to enhance desired properties by adding small concentrations of selected LDHs.

The authors thank Dr. Rafael Marangoni (DQ/UFPR) for help in the synthesis of LDHs.

References

1. Pinnavaia, T.; Beall, G. Polymer-Clay Nanocomposites; Wiley: Chichester, England, 2001.
2. Costache, M.; Wang, D.; Heidecker, M.; Manias, E.; Wilkie, C. Polym Adv Technol 2006, 17, 272.
3. Grunlan, J.; Grigorian, A.; Hamilton, C.; Mehrabi, A. J App Polym Sci 2004, 93, 1102.
4. Gilman, J.; Jackson, C.; Morgan, A.; Harris, R.; Manias, E.; Gianellis, E.; Wuthenow, M.; Hilton, D.; Phillips, S. Chem Mater 2000, 12, 1866.
5. Leroux, F.; Meddar, L.; Mailhot, B.; Morlat-Thérias, S.; Gardette, J. Polymer 2005, 46, 3571.
6. Liu, P.; Gong, K.; Xias, P.; Xiao, M. J Mater Chem 2000, 10, 933.
7. Alexandre, M.; Dubois, P. Mater Sci Eng R 2000, 28, 1.
8. Xu, Z.; Braterman, P. Appl Clay Sci 2010, 48, 235.
9. Wypych, F.; Satyanarayana, K. J Colloid Interface Sci 2005, 285, 532.
10. Wang, G.; Wang, C.; Chen, C. J Inorg Organomet Polym Mater 2005, 15, 239.
11. Tseng, C.; Hsueh, H.; Chen, C. Compos Sci Technol 2007, 67, 2350.
12. Berti, C.; Fiorini, M.; Sisti, L. Eur Polym Mater 2009, 45, 70.
13. Nyambo, C.; Songtipya, P.; Manias, E.; Jimenez-Gasco, M.; Wilkie, C. J Mater Chem 2008, 18, 4827.
14. Nogueira, T.; Gonçalves, M.; Lona, L.; Vivaldo-Lima, E.; McManus, N.; Penlidis, A. Adv Polym Technol 2010, 29, 11.
15. Nogueira, T.; Lona, L.; McManus, N.; Vivaldo-Lima, E.; Penlidis, A. J Mater Sci 2010, 45, 1878.
16. Wang, G.; Wang, C.; Chen, C. Polymer 2005, 46, 5065.
17. Xu, Z.; Braterman, P.; Yu, K.; Xu, H.; Wang, Y.; Brinker, C. Chem Mater 2004, 16, 2750.
18. Nakanishi, K.; Solomon, P. Infrared Absortion Spectroscopy; Holden-Day: San Francisco, USA, 1977.
19. Matusinovic, Z.; Rogosic, M.; Sipusic, J. Polym Degrade Stab 2009, 94, 95.
20. Ding, Y.; Gui, Z.; Zhu, J.; Hu, Y.; Wang, Z. Mater Res Bull 2008, 43, 3212.
21. Liu, Y.; Hsu, C.; Hsu, K. Polymer 2005, 46, 1851.
22. Monteiro, S.; Rodriguez, R.; Lopes, F.; Soares, B. Tecnologia em Metalurgia e Materiais 2008, 5, 111 (in Portuguese).
23. Marangoni, R.; Taviot-Guého, C.; Illaik, A.; Wypych, F.; Leroux, F. J Colloid Interface Sci 2008, 326, 366.